Protonation of S 4 , S 6 , and S 8 Sulfur Cycles. A Quantitative Study

6 **AUTHORS**, INCLUDING:

M'hamed Esseffar
Cadi Ayyad University
79 PUBLICATIONS **947** CITATIONS

SEE PROFILE

Otilia Mó
Universidad Autónoma de Madrid
402 PUBLICATIONS **6,371** CITATIONS

SEE PROFILE

Protonation of S₄, S₆, and S₈ Sulfur Cycles. A Quantitative Study

J.-L. M. Abboud,*,† M. Esseffar,‡ M. Herreros,† O. Mó,‡ M. T. Molina,§ R. Notario,† and M. Yáñez*,‡

Instituto de Química Física Rocasolano, C.S.I.C. Serrano 119, E-28006 Madrid, Spain, Departamento de Química, C-9, Universidad Autónoma de Madrid, Cantoblanco, E-28049 Madrid, Spain, and Instituto de Química Médica, C.S.I.C., Juan de la Cierva, 3, E-28006 Madrid, Spain

Received: February 16, 1998

We have determined the gas-phase basicities of S_6 and S_8 by means of Fourier transform ion cyclotron resonance spectroscopy (FT-ICR): 167.8 and 187.1 kcal/mol, respectively. An ab initio investigation of the local minima of the S_6H^+ potential energy surface shows that the most stable protonated species corresponds to a distorted five-membered ring structure rather than to a six-membered ring species. When the final energy of the aforementioned protonated species is evaluated at the G2(SVP,MP2) level, the agreement with the experimental value is very good. A G2(MP2) survey of the S_4 and S_4H^+ potential energy surfaces shows that the most stable neutral and protonated species present cis open-chain structures. The relative stabilities of the different species investigated are extremely sensitive to electron correlation effects. At the G2(MP2) level S_4 is predicted to be slightly more basic than S_6 in the gas phase. Some preliminary ab initio calculations on the most probable structures of S_8H^+ are also reported.

Introduction

One of the topics in the gas-phase ion chemistry which received a great deal of attention in the last two decades is the determination of association energies of different neutrals with different kinds of cations. In this way it was possible to define basicity scales[1] not only with respect to the proton but also with respect to other cations.[2] The basicities so defined are generally describes as intrinsic basicities or, in general, intrinsic reactivities, because they are not masked by solvent effects. Often the neutrals exhibit unexpected gas-phase reactivities associated with the formation of nonclassical structures,[3,4] which will not be stable in the condensed phase, or with the fission of some chemical bonds of the base, as is the case of the dissociative proton attachment processes of fluoro- and chloroalkanes,[5] which lead to the loss of XH (X = F,Cl) or the protonation of highly strained species, as tetraphosphacubane,[6] which results in a partial breaking of the cubic structure of the neutral.

Our groups have been recently involved in the study of the intrinsic basicities or acidities of strained systems,[4,6−10] containing first- and second-row atoms as active centers. Along these lines, the aim of this paper is the study of sulfur cyclic forms and their intrinsic basicities, both from the experimental and the theoretical point of view. The first candidate is obviously S_6, which is a stable species amenable to experimental work. A survey of the potential energy surface corresponding to the protonated forms S_6H^+ shows the existence of quite stable unexpected structures, whose rationalization will be one of our goals. For the particular case of S_8H^+ species, we will present some preliminary ab initio calculations, because the size of these systems renders the use of high-level ab initio techniques unaffordable. In this respect it must be mentioned that very little is known regarding the gas-phase reactivity of these cycles and we are only aware of the study of the gas-phase reactions between S_8 and Ca^+, where the formation of $[CaS_3]^+$ and $[CaS_{11}]^+$ was reported.[11] We have considered it also of interest to carry out a parallel characterization of the potential energy

surface (PES) associated with a smaller cycle of the series, the S_4H^+ protonated species. Although the survey of the S_4H^+ PES can be only done on theoretical grounds, their most significant features may help in establishing common trends to sulfur cycles of different size.

Experimental Section

Materials. *S₈.* A highly pure sample of cyclooctasulfur (99.99%, Aldrich) was used. lts purity was assessed by means of its mass spectrum.
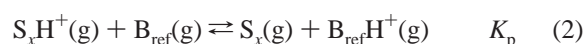
S₆. Cyclohexasulfur was obtained, according to Schmidt and co-workers,[12] by treating bis(cyclopentadienyl)titanium penta-sulfide with sulfur dichloride in CS_2 at 0 °C in the dark. The product was further crystallized from cold CS_2 in the dark, dried, and immediately subject to the FT-ICR study. Again, purity was assessed by means of the mass spectrum.

FT-ICR Spectrometer. The instrument is a modified Bruker CMS 47 FT-ICR mass spectrometer[13] used in previous studies.[4−8,14,15] A detailed description of the main features of this instrument are given in refs 4, 13, and 14. The substantial field strength (4.7 T) of its supraconducting magnet allows the monitoring of ion−molecule reactions for relatively long periods of time.

Determination of the Gas-Phase Basicities. The gas-phase basicity of the species S_x ($x = 6, 8$), $GB(S_x)$ is defined as the standard Gibbs energy change for reaction 1, while the corresponding proton affinity, $PA(S_x)$, is the standard enthalpy change for the same process:

$$S_xH^+(g) \rightarrow S_x(g) + H^+(g) \qquad (1)$$

The equilibrium constants K_p for the proton exchange between $S_x(g)$ and a series of reference bases B_{ref}, reaction 2,

$$S_xH^+(g) + B_{ref}(g) \rightleftharpoons S_x(g) + B_{ref}H^+(g) \qquad K_p \quad (2)$$

Protonation of S₄, S₆, and S₈ Sulfur Cycles

J. Phys. Chem. A, Vol. 102, No. 41, 1998 **7997**

were experimentally determined in the FT-ICR spectrometer indicated above.

As in previous studies,[4,6−8,14a,15] K_p values were obtained by means of an experimental technique based on that used in Prof. Taft's laboratory.[16,17] In these experiments, mixtures of $B_{ref}(g)$ and $S_x(g)$ of known partial pressures (total pressures generally in the range 5×10^{-7} to 3×10^{-6} mbar) were ionized by electron impact (nominal energies in the range $12-15$ eV). $S_xH^+(g)$ and $B_{ref}H^+(g)$ were obtained by means of chemical ionization, the proton sources being the ionic fragments of $B_{ref}(g)$. The ionic fragments were deprotonated in $2-3$ s, the system being monitored for an extra $10-20$ s. A constant ratio of the intensities of the relevant ions, $S_xH^+(g)$ and $B_{ref}H^+(g)$ was reached after ca. 5 s and remained constant until the end of the experiment. During the first few seconds, samplings were carried out every $0.2-0.3$ s and, afterward, every 0.5 s.

The reversibility of reaction 2 was confirmed by means of double-resonance- like experiments.[4]

K_p values, defined through eq 3, were obtained by combining the ratio of the intensities of $B_{ref}H^+$ to S_xH^+ (taken as a measure of the ratio of the partial pressures of these ions) with the ratio of the partial pressures of the neutral reagents.

$$K_p = [P(S_x)/P(B_{ref})] \, [P(B_{ref}H^+)/P(S_xH^+)] \qquad (3)$$

The corresponding values of the latter, as measured by the Bayard−Alpert gauge, were corrected following Bartmess and Georgiadis[18] by means of the correlation between the relative sensitivities determined with the gauge (relative to nitrogen) and the polarizabilities of the various materials. The latter were estimated using Miller's values.[19]

Because of the high accuracy of the ratios of ion intensities it provides, the McIver−Gaumann[20] fast sweep/cross-correlation method was used, as in most of our previous studies.

Computational Details

Standard ab initio calculations, to characterize the minima of the S₄, S₄H⁺, S₆, and S₆H⁺ potential energy surfaces, have been carried out by using the Gaussian94 series of programs.[21]

The geometries of the different species under investigation have been fully optimized at the HF/6-31G(d) level. The corresponding harmonic vibrational frequencies were calculated at the same level of theory using analytical second derivative techniques. With the set of harmonic vibrational frequencies, it was possible to characterize the stationary points of the PES as minima or saddle points and to calculate the zero-point energies (ZPE) which were scaled by the empirical factor 0.893.

The geometries so obtained were then refined at the MP2-(Full)/6-31G(d) level. It is something well established that correlation effects must be included in the theoretical treatment to get reliable geometries. We would like to emphasize here that this is particularly true when dealing with sulfur-containing compounds,[15,22−24] because, as we shall show later, several HF local minima were found not to be stable at the MP2 level. In some critical cases, which will be discussed later, the MP2 geometries were further refined at the QCISD/6-311G(d) level.

As it was found for other strained systems as P₄ and tetra-*tert*-butyl-tetraphosphacubane, reliable proton affinities (i.e., proton affinities in good agreement with experimental values), which can be only attained at high ab initio leveIs.[4,6] For this purpose the Gaussian-2 theory[25] has been proved to be a very suitable method. Since a treatment of systems as large as S₆H⁺ at the G2 level is still prohibitively expensive, we have used the more economic G2(MP2) formalism[26] where the energy

enhancements associated to high-angular momentum basis and diffuse basis are obtained at the MP2 level. For the S₆ and S₆H⁺ conformers the more economic G2(SVP,MP2) scheme,[27] where the QCISD(T) component of the final energy is evaluated using a split-valence (SPV) 6-31G(d) basis sets, was adopted. The resulting total energies are effectively of a QCISD(T)/6-311+G(3df,2p) quality.

The bonding of the different neutral and protonated species under consideration was analyzed using two different electron population techniques, namely, the natural bond orbital (NBO) method of Weinhold et al.[28] and the atoms-in-molecules (AIM) theory of Bader and co-workers.[29−31] The first formalism allowed us to obtain the atomic natural total charges and a description of the bonding in terms of the natural hybrids centered on each atom. Using the second approach we have located the bond critical points (bcp) (i.e., points where the electron density function $\rho(\mathbf{r})$ is a minimum along the bond path and maximum in the other two directions). At the same time, the determination of the bond paths i.e., the zero-flux lines connecting the different atomic basins of the molecule, makes it possible to have a good description of the strain of the system, by comparing the bond path angles with the geometrical bond angles. We have also evaluated the Laplacian of the density, $\nabla^2\rho(\mathbf{r})$. As has been shown in the literature,[31] the Laplacian identifies regions of the space wherein the electronic charge is locally depleted ($\nabla^2\rho > 0$) or built up ($\nabla^2\rho < 0$). The former situation is typically associated with interactions between closed-shell systems (ionic bonds, hydrogen bonds, and van der Waals molecules), while the latter characterizes covalent bonds, where the electron density concentrates in the internuclear region. There are however some exceptions to this general rule, mainly when the atoms involved in the bond are very electronegative. Hence, we shall use in our discussion the energy density,[32] $H(\mathbf{r})$. In general, negative values of $H(\mathbf{r})$ imply a stabilizing charge concentration typically associated with covalent interactions, while for essentially electrostatic interactions the value of this index is positive.

Results and Discussion

1. Experimental Results. For each reference base, GB(S$_x$) is obtained through eq 4:

$$GB(S_x) = GB(B_{ref}) + \delta\Delta G^oH^+ \qquad (4)$$

wherein

$$\delta\Delta G^oH^+ = -RT \ln K_p$$

The experimental results are given in Table 1. Each equilibrium constant is the average of at least six runs at different total pressures. Also, the ratios of the pressures were varied as widely as possible. GB(B$_{ref}$) values are taken from the very recent critical compilation by Hunter and Lias.[17c]

The uncertainties on K_p values can be estimated at ca. 30%, part of it originating in the reproducibility (15%) of the experiments and the remaining, in the correction of the ion gauge data. This amounts to $RT \ln(1.3)$, that is, 0.18 kcal/mol in Gibbs energy. The contribution to uncertainty originating in GB(B$_{ref}$) is relatively small, thanks to the multiple overlap method used to link the GB values and can be estimated at ca. $0.1-0.3$ kcal/mol.

From the experimental data given above, average values of 167.8 and 187.1 kcal/mol obtain for GB(S₆) and GB(S₈), the corresponding standard deviations being 0.3 and 0.2 kcal/mol.
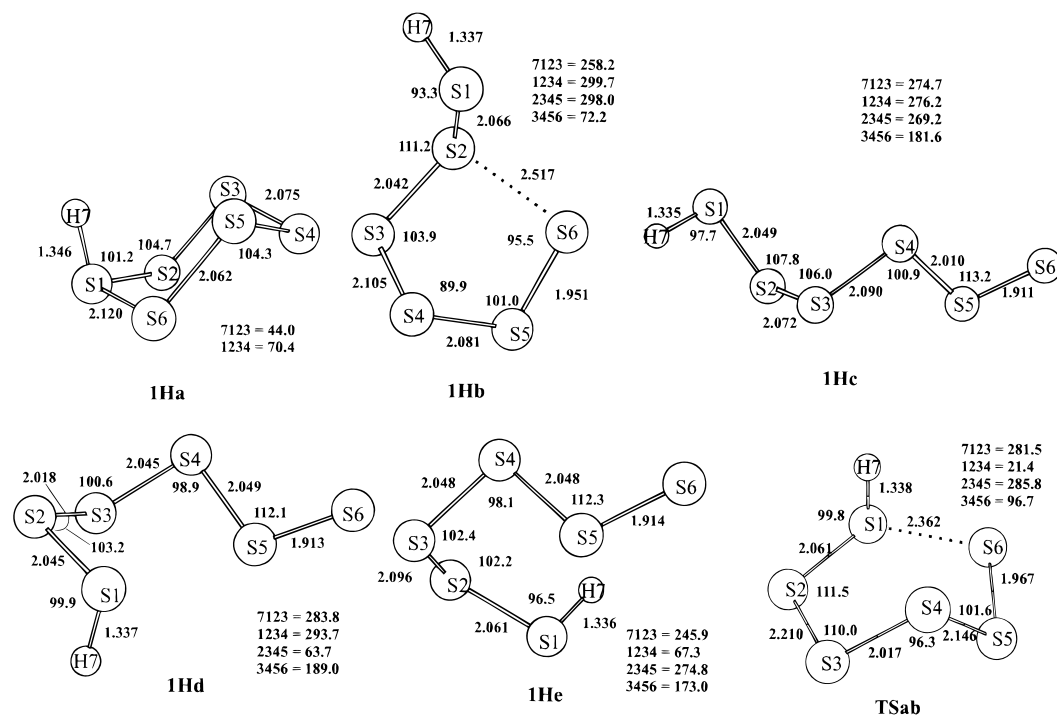
Figure 1. MP2(full)/6-31G(d) optimized geometries of the protonated forms of S_6. Bond lengths in angstroms and bond angles in degrees. For each optimized structure, the most relevant dihedral angles in degrees are also given.

According to the IUPAC criterion,[33] the latter measure the precision of these values.

2. S_6 and S_6H^+ Potential Energy Surfaces. Because one of the main objectives of our work was an unambiguous characterization of the protonated form of S_6, the first step of our theoretical survey concentrates on this particular problem. It seems well established, both experimentally[34] and theoretically,[22] that the structure of S_6 corresponds to a chair-shaped six-membered ring, the boat-shaped conformation being about 14 kcal/mol less stable.[22] It is likely that a similar chair-shaped structure should be expected for the corresponding protonated form. Our calculations showed indeed that this structure, namely, **1Ha** (See Figure 1) was a minimum of the corresponding PES at the HF/6-31G(d) level of theory. However, the stability of this protonated species was smaller than that expected from the measured proton affinity of S_6. This disagreement between theory and experiment prompted us to investigate other possible structures for the S_6H^+ species. A systematic searching of all the possible conformers leads to the local minima depicted in Figure 1. The most important finding was that the global minimum of the PES was the **1Hb** species rather than **1Ha**. Also, the other conformers were not far in energy from **1Ha** (See Table 2). One may wonder then, whether species **1Hb**, which has a five-membered ring would be the result of the protonation of a similar neutral species **1b**. Because in the studies reported in the literature this particular conformation was never considered, we thought it of interest to investigate whether it corresponds to a local minimum. For the sake of completeness we have included in our calculations also the chair-shaped six-membered ring, **1a**, because its geometry was only described at the HF level,[22] as well as the structure containing a four-membered ring, namely, **1c**, and different open-chain conformations, **1d** and similar (See Figure 2). Our results showed that none of these conformers was actually stable. Indeed, although a **1b** local minimum was found at the HF level, it dissociated to three S_2 molecules when its geometry was refined at the MP2 level. Structure **1c** dissociates, already at

TABLE 1: Experimental Results Pertaining to the determination of $GB(S_6)$ and $GB(S_8)^a$

			(a) $GB(S_6)$		
ref	$GB(B_{ref})^b$	$\delta\Delta G_{H+}$	$GB(S_6)$	$GB(S_6)$ (av)
Cl_3CCH_2OH	167.3	0.2	167.5	
				167.8 ± 0.3
Cl_3CCN	166.1	1.9	168.0	
				$(175.6 \pm 0.3)^c$

			(b) $GB(S_8)$		
ref	$GB(B_{ref})^b$	$\delta\Delta G_{H+}$	$GB(S_8)$	$GB(S8)$ (av)
$tert$-C_4H_9CN	186.2	0.8	187.0	
C_6H_5CN	186.4	0.6	187.0	
				187.1 ± 0.2
				$(193.8 \pm 0.2)^d$
$(CH_3)_2CO$	186.9	0.4	187.3	

^{a} All values in kcal/mol. ^{b} From ref 17c. ^{c} The value in parentheses corresponds to the proton affinity estimated using the entropy changes calculated at the HF/6-31G(d) level. ^{d} The value in parentheses corresponds to the proton affinity estimated using the entropy changes calculated at the HF/3-21G(d) level.

the HF level, to a S_4 cyclic subunit and a S_2 molecule. Similarly, all attempts to obtain stable S_6 open chains led to a dissociation of the system into three S_2 molecules. Hence, taken into account that the other stable conformers of S_6 are about 14 kcal/mol less stable than the global minimum,[22] we must conclude that all possible minima of the S_6H^+ PES arise from a unique neutral species, **1a**.

2.1. Structures and Bonding. The optimized structures of S_6 protonated species are given in Figure 1. As expected in the neutral chair-shaped conformer, all S−S bonds are strictly equivalent, with bond lengths of 2.078 Å, and S−S−S bond angles of 102.8°.

In general, protonation implies a sizably large charge transfer to the incoming proton, which usually comes from the valence shell of the basic center and from the bonds in which it participates.[35] In the particular case of S_6 molecule, protonation

Protonation of S$_4$, S$_6$, and S$_8$ Sulfur Cycles

J. Phys. Chem. A, Vol. 102, No. 41, 1998 **7999**

TABLE 2: Total Energies, *E* (hartree), Relative Energies, Δ*E* (kcal/mol), and Proton Affinities, PA (kcal/mol), for the Relevant Species

system	E					ΔE			PA		
			QCISD(T)								
	HF	MP2	6-311G(d)	6-311+G(df)	G2(MP2)	HF	MP2	G2(MP2)	HF	MP2	G2(MP2)
1	−2385.047 78	−2385.840 97			−2386.475 20[c]	0.0	0.0	0.0	167.6	174.0	177.9[c]
1Ha	−2385.322 61	−2386.122 30			−2386.753 60[c]	0.0	0.0	0.0			
1Hb	−2385.311 20	−2386.124 96			−2386.756 44[c]	6.5	−2.3	−1.8[c]			
1Hc	−2385.291 34	−2386.118 28				12.4	1.7				
1Hd	−2385.301 13	−2386.121 32				15.8	−0.6				
1He	−2385.297 65	−2386.117 80				19.8	2.0				
TSab	−2385.283 06	−2386.091 74				24.8	19.2				
2	−1589.977 94	−1590.496 68			−1590.923 51	0.0	0.0	0.0	166.5	172.5	
3	−1589.955 36	−1590.501 63			−1590.930 85	14.0	−3.2	−4.6	192.7	187.9	
4	−1589.944 65	*a*	−1590.609 53		−1590.939 17	20.8	−9.8				
5	−1589.925 55	−1590.573 73	−1590.615 77	−1590.803 51		32.9	−48.5				
6	−1589.956 45	*b*	−1590.623 77	−1590.808 71	−1590.955 23	13.5		−19.9			182.9
2H	−1590.248 98	−1590.777 35			−15901.201 66	19.8	33.0	25.2			
3H	−1590.269 31	−1590.807 94			−1591.230 43	6.2	13.0	7.2			
4H	−1590.279 35	−1590.828 72			−1591.241 86	0.0	0.0	0.0			
6H	−1590.279 12	−1590.832 82			−1591.244 51	0.3	−2.5	−1.6			

a The *trans* isomer dissociates to two S$_2$ molecules at the MP2 level. *b* The *cis* isomer collapses to the *D*$_{2h}$ rectangular isomer **5** at the MP2 level. *c* Values obtained at the G2(SVP,MP2) level.
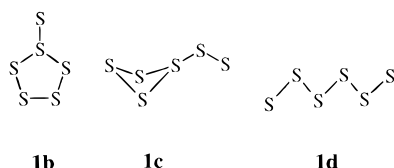
Figure 2. Non-chair-shaped six-membered ring conformers of S$_6$, examined in this work.

at one of the sulfur atoms may lead to two different electron density rearrangements.

The proton attachment to S1 of **1a** to yield **1Ha** results in an enhancement of the electronegativity of this atomic center which depopulates equally the two bonds (S1−S2 and S1−S6) in which it participates. As a consequence, both linkages become weaker and longer. S2 and S6, in turn, polarize the bonding charge density at the S2−S3 and S6−S4 linkages toward them. This implies an increase of the charge density at the bcps and a reinforcement of the bonds, which become shorter. This charge redistribution is also reflected in the natural charges, which show that the positive charge is clearly dispersed within the ring, even though the protonated sulfur atom is the one which has the largest positive charge.

However, an alternative mechanism is possible where the enhanced electronegativity of S1 is satisfied by depopulating specifically one of the S−S linkages (S1−S6 in the figure), which eventually dissociates. Once this bond has been broken, the resulting open chain can fold in different ways yielding the **1Hb**, **1Hc**, **1Hd**, and **1He** species. It is worth noting that all these species, with the only exception of **1Hb**, have a common feature, in the sense that all of them have an almost planar S$_4$ moiety (S3−S4−S5−S6 in the figure), to which the S$_2$H subunit is attached in different relative orientations. Furthermore, the local structures of the S$_4$ moieties, in terms of bond lengths and bond angles, are also rather similar in all cases. In particular, it can be observed that the terminal S5−S6 linkage have a noticeable double-bond character, which is reflected in a shorter bond length. This can be understood taking into account that the fission of the S1−S6 bond and the formation of the new S1−H linkage leaves S6 as an electron deficient atom. In other words, the protonation processes can be visualized as follows: one of the lone pairs of S1 becomes engaged in the formation of the new covalent linkage with the incoming proton. Then S1 recovers the lost charge by pulling the bonding pair associated with the S1−S6 linkage, leaving S6 formally with the positive charge. The fact that S6 becomes electron deficient favors the lone-pair donation from the closest sulfur (S5). The double-bond character of this linkage is confirmed by the NBO analysis which shows the existente of two bonding MOs involving S5 and S6. Consistently, the charge density at the bcp (≈ 0.19 *e* au^{-3}) is much larger than that found in typical S−S single bonds (≈ 0.13 *e* au^{-3}) (See Table 3).

The bonding characteristics of species **1Hb** are slightly different, in the sense that the electron deficient S6 atom interacts also with S2. In other words, in **1Hb** species the chain folds approaching the electron deficient S6 sulfur atom to S2. This favors the lone-pair donation from S2 to S6 and hence the formation of a weak linkage between both atoms. Actually, the NBO analysis shows the existentence of a bonding MO between both centers, with a dominant participation (71%) from the hybrids centered at S2. Consistently, a bcp with a charge density about half (0.06 *e* au^{-3}) that of a typical S−S single bond is found in the S2−S6 bonding region. This additional bonding interaction contributes to stabilize this form which becomes accordingly the global minimum of the PES.

2.2. Relative Stabilities and Proton Affinities. The total and relative energies of the different protonated forms of S$_6$ are given in Table 2. The first conspicuous fact is that, as it was found for the neutral species,[22] the calculated relative stabilities of the S$_6$ protonated structures are quite sensitive to electron correlation effects. At the HF level, the species **1Ha** is predicted to be the global minimum of the PES, while at the MP2 level is found to lie 2.3 kcal/mol above species **1Hb**. Also the relative stabilities of species **1Hc** and **1He** are reversed when including electron correlation effects. It is also worth noting that the energy gaps between the different conformers decrease significantly when electron correlation effects are included. Also importantly, the gap between species **1Ha** and **1Hb** changes only slightly when obtained at the G2(SVP,MP2) level, which allow us to conclude that the global minimum of the PES is indeed the **1Hb** species.

These changes in relative stabilities have a dramatic effect on the calculated proton affinities. As shown in Table 2 the HF value differs of the experimental one by more than 7 kcal/

TABLE 3: Bonding Characteristics[a] and Natural Atomic Charges. The Values of the Charge Densities (ρ) and the Energy Densities ($H(\mathbf{r})$) at the bcps are in au

S6 derivatives	S1–S2 ρ	S1–S2 $H(\mathbf{r})$	S2–S3 ρ	S2–S3 $H(\mathbf{r})$	S3–S4 ρ	S3–S4 $H(\mathbf{r})$	S4–S5 ρ	S4–S5 $H(\mathbf{r})$	S5–S6 ρ	S5–S6 $H(\mathbf{r})$	S6–S1 ρ	S6–S1 $H(\mathbf{r})$	S1–H7 ρ	S1–H7 $H(\mathbf{r})$	S1	S2	S3	S4	S5	S6	H7
1Ha	0.128	−0.062	0.143	−0.079	0.141	−0.076	0.141	−0.076	0.143	−0.079	0.128	−0.062	0.225	−0.212	+0.373	+0.113	+0.096	+0.093	+0.096	+0.113	+0.115
1Hb	0.143	−0.080	0.149	−0.086	0.130	−0.064	0.140	−0.074	0.176	−0.126	0.060[b]	−0.010[b]	0.223	−0.218	+0.019	+0.289	+0.083	+0.070	+0.253	+0.185	+0.100

S4 derivatives	S1–S2 ρ	S1–S2 $H(\mathbf{r})$	S2–S3 ρ	S2–S3 $H(\mathbf{r})$	S3–S4 ρ	S3–S4 $H(\mathbf{r})$	S4–S1 ρ	S4–S1 $H(\mathbf{r})$	S–H ρ	S–H $H(\mathbf{r})$	S1	S2	S3	S4	H
2	0.129	−0.062	0.129	−0.062	0.129	−0.062	0.129	−0.062							
3	0.103	−0.038	0.126	−0.062	0.189[c]	−0.156[c]					+0.730	−0.100	−0.100	−0.529	
4	0.172	−0.122	0.134	−0.067	0.172	−0.122	0.013	0.003			−0.141	+0.141	+0.141	−0.141	
5	0.175	−0.124			0.175	−0.124	0.122	−0.056			−0.133	+0.133	+0.133	−0.133	
6	0.177	−0.129	0.121	−0.054	0.177	−0.129									
2H	0.122	−0.056	0.122	−0.061	0.129	−0.061			0.224	−0.207	+0.429	+0.180	+0.180	+0.180	+0.129
3H	0.139	−0.077	0.120	−0.055	0.144[c]	−0.081[c]			0.219	−0.207	+0.601	+0.123	+0.123	+0.028	+0.124
4H	0.145	−0.082	0.156	−0.094	0.186	−0.151			0.224	−0.219	+0.048	+0.109	+0.744	+0.006	+0.092
6H	0.150	−0.089	0.149	−0.085	0.187	−0.153			0.223	−0.216	+0.015	+0.198	+0.476	+0.122	+0.189

[a] The values of ρ and $H(\mathbf{r})$ for the chair-shaped conformer of S6 (**1a**) are 0.140 and −0.074 au, respectively. [b] These values correspond to the S2–S6 bond critical point. [c] These values correspond to the S1–S4 bond critical point.

mol, while at the MP2 level the difference between experimental and calculated proton affinities is drastically reduced, the MP2 estimated value being 1.6 kcal/mol lower than the experimental figure. When the estimated theoretical value is obtained, including correlation effects beyond fourth order and using large basis sets, the agreement between theory and experiment is similarly good, and the G2(MP2) estimate is 2.3 kcal/mol higher than the experimental one.

Unfortunately, it is not possible to establish, from an experimental point of view, which is the actual structure of the protonated form of S_6. On the other hand, the energy gap between species **1Ha** and **1Hb** at the G2(SVP,MP2) level is not large enough to allow us to assume that the structure **1Hb** will be the only one present in the gas phase. However, the transition state (**TSab** in Figure 1) which connects both protonated species is quite high in energy with respect to any of them. Hence, in principle, an easy interconversion between both protonated forms under normal experimental conditions seems unlikely.

3. S_4 and S_4H^+ Potential Energy Surfaces. The relative stabilities of the different local minima of the S_4 PES have been the subject of some controversy.[22,23] Raghavachari et al.[22] found that the relative stability of the D_{2h} rectangular and the C_{2v} cis isomers oscillates with the order of perturbation theory, the former being slightly more stable than the latter at the QCISD-(T)/6−31G(d)//HF/3-21G(d) level of theory. In this respect it is worth noting that the cis conformer is not stable at the MP2 level, because it collapses to the rectangular D_{2h} isomer.[22] In contrast, Quelch et al.[23] found that a MR−CISD treatment with generalized quadruples correction predicts the rectangular isomer to be 1.8 kcal/mol less stable than the cis one. Furthermore, the D_{2h} rectangular isomer was found to be a transition state at the CISD level.

Because the characterization of the most stable neutral and protonated forms is crucial for our purposes we have estimated the relative energies of the different S_4 and S_4H^+ conformers at the G2(MP2) level. Taking into account that, for the particular case of the cis, trans, and rectangular isomers, because correlation effects beyond second order seem to be crucial, the structures of these three species were optimized at the QCISD/6-311G(d) level rather than at the standard MP2/6-31G(d) level. The optimized structures of the S_4 and S_4H^+ stationary points are given in Figure 3 Their total energies have been included in Table 2.

At the QCISD/6-311G(d) level, the cis S_4 conformer is predicted to be 5.3 and 8.9 kcal/mol more stable than the rectangular and the trans isomers, respectively. More importantly, while at this level the cis and the trans isomers are local minima of the PES, the rectangular isomer has two imaginary frequencies (1500i cm^{-1} and 231i cm^{-1}) which correspond to the two possible S−S out-of-phase stretching combinations (S1−S2 + S3−S4 and S1−S3 + S2−S4), respectively. Because Raghavachari et al.[22] pointed out that the inclusion of triples correction favors the stability of the rectangular isomer with respect to the cis one, we have calculated the energies of these two structures using the QCISD(T) formalism together with two different basis set expansions, namely, 6-311G(d) and 6-311+G(df). As shown in Table 2, at both levels of theory the cis isomer is still the most stable one.

The puckered four-membered ring (**2**) and the branched ring (**3**) isomers were also found to be stable at the MP2 level, although they are predicted to be 19.9 and 15.3 kcal/mol less stable, respectively, than the cis conformer, at the G2(MP2) level. The S_4 open-chain species was found to be a local minimum at the HF level, but it dissociates to two S_2 molecules

Protonation of S$_4$, S$_6$, and S$_8$ Sulfur Cycles

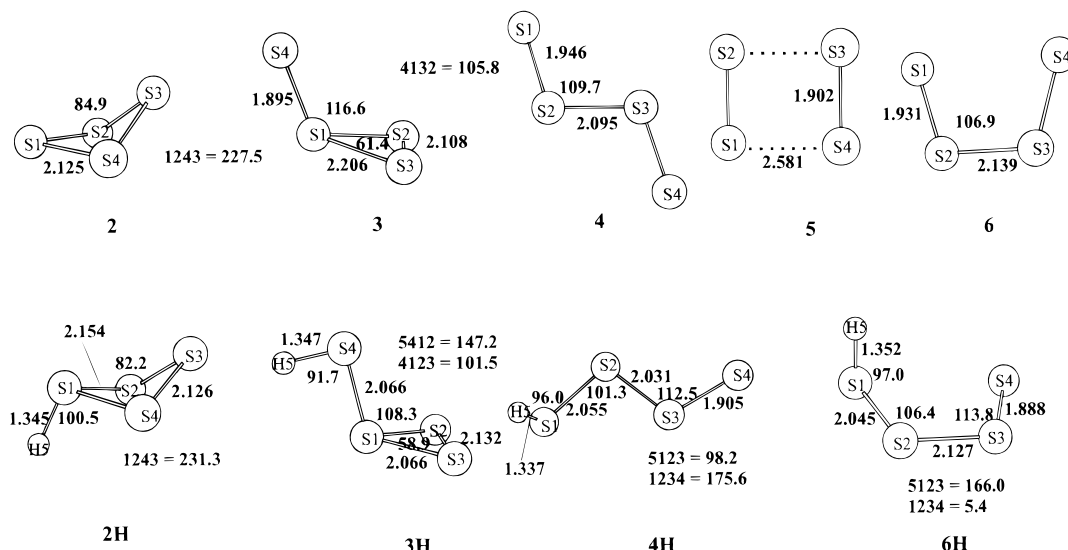*J. Phys. Chem. A, Vol. 102, No. 41, 1998* **8001**

Figure 3. MP2(full)/6-31G(d) optimized geometries of the protonated forms of S$_4$. Bond lengths in angstroms and bond angles in degrees. For each optimized structure, the most relevant dihedral angles in degrees are also given. For species **4**−**6**, the reported geometries were obtained at the QCISD/6-311G(d) level. For species **2** and **2H**, the S2S1S4 bond path angles (in degrees) are 87.9 and 88.4, respectively. For species **3** and **3H** the bond path angles (in degrees) are as follows: S1S2S3, 72.3 and 73.3; S3S1S2, 71.2 and 73.1.

when its geometry was refined at the MP2 level. This is not the case for the corresponding protonated species where the open-chain protonated forms **4H** and **6H** are quite stable, the latter being the global minimum of the PES. Our results show the existence of other two conformers, **2H** and **3H**, which arise from the protonation of species **2** and **3**, respectively.

3.1. Structures and Bonding. The bonding characteristics of the S$_4$ and S$_4$H$^+$ stable systems have been summarized in Table 3. It can be seen that the charge densities at the S−S bcps of **2** are slightly smaller than those found for **1**. Consistently, the corresponding bonds are longer. This is a direct consequence of the higher strain of the S$_4$ cycle, as indicated by the difference between bond path angles and geometrical angles (see Figure 3). As it was found for the six-membered ring, protonation of **2** at S1 leads to a decrease of the electron density at the S1−S2 and S1−S4 bcps which is mirrored in a lengthening of both linkages. Also the puckering of the ring decreases from 132.5° to 128.7°.

S1 in species **3** has a hypervalent character since according to the topological analysis of $r(\mathbf{r})$, the S1−S4 linkage has a charge density at the bcp typical of S=S double bonds. The bonds of the three-membered ring are weaker than normal S−S bond lengths as it should be expected from a highly strained system. This is also evidenced by the significant differences between bond path angles and geometrical angles (see Figure 3). As expected, protonation of **3** at S4 implies a significant lengthening of the S4−S1 bond which loses its double-bond character, while the S1−S2 and S1−S3 linkages become reinforced. This is a direct consequence of the hybridization changes that take place upon protonation. Upon protonation, S4 depopulates the S4−S1 bond and this produces an enhancement of the electronegativity of S1. This is reflected in an increase of the s character of the hybrids which participate in the S1−S2 and S1−S3 bonds, which accordingly become shorter. Protonation at S2 implies an analogous process, in the sense that S2 depletes charge from the weaker S1−S2 bond to recover the charge transferred to the incoming proton. Because the charge density at the S1−S2 bonding region was already low, the aforementioned depletion leads to the fission of the bond, yielding the open-chain structure **4H**. Of course structure **4H** can be also formed by a direct protonation of the trans
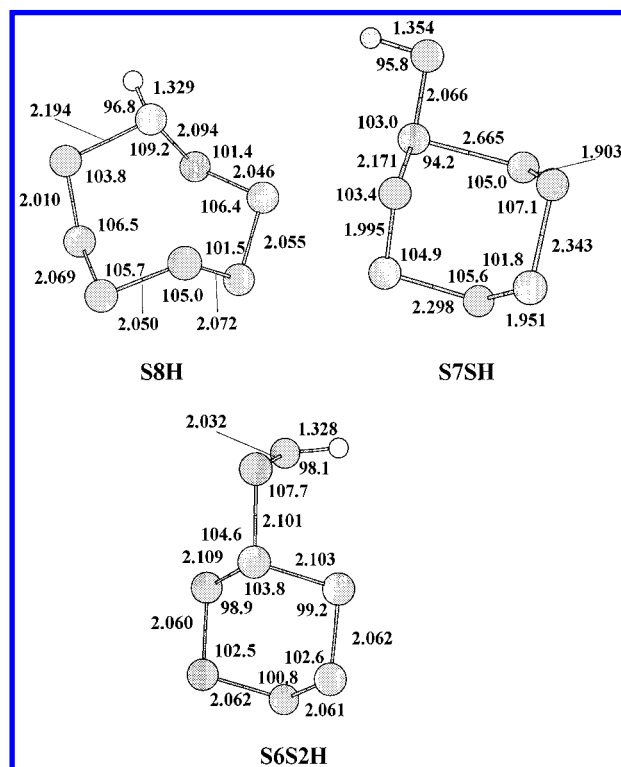

Figure 4. HF/3-21G(d) optimized geometries of S$_8$H$^+$ cyclic species. Bond lengths in angstroms and bond angles in degrees.

conformer **4**. The charge redistribution which follows is similar to that describes before and results in a reinforcement of the S2−S3 and S3−S4 bonds, while the S1−S2 linkage becomes weaker (see Table 3) and longer (see Figure 3). Similar effects appear when the cis isomer **6** becomes protonated to yield structure **6H**. It is worth mentioning that this protonated form is also the product of the protonation of the D_{2h} rectangular isomer, because the charge polarization induced by the proton results in a noticeable increase of the S2−S3 bonding interaction.

3.2. Relative Stabilities and Proton Affinities. As it was found previously for the neutrals,[22,23] the relative stabilities of S$_4$H$^+$ species are very sensitive to electron correlation effects. As shown in Table 2, at the HF level species **4H** is predicted

TABLE 4: Total Energies (*E*, hartree), zero-point energies (ZPE, hartree) for the S_8H^+ Species Investigated. Values within Parentheses Correspond to the Calculated Proton Affinities in kcal/mol

system	HF/6-31G(d)//HF/3-21G(d)	ZPE	MP2/6-31G(d)//HF/3-21G(d)	MP2/6-311+G(3df,2p)//HF/3-21G(d)
S8	−3180.075 75	0.013 98	−3181.051 69	−3181.740 46
S8H	−3180.337 34 (160.1)	0.023 83	−3181.317 73	
S7SH	−3180.301 15	0.022 64	−3181.320 81 (165.5)	−3182.022 54 (173.7)
S6S2H	−3180.336 23	0.023 09	−3181.313 56	

to be the global minimum, while at the MP2 level it is found to lie 2.5 kcal/mol above species **6H**. A similar result is found at the G2(MP2) level which predict the latter to be 1.6 kcal/mol more stable than the former. The energy gaps between the global minimum and the remaining protonated conformers are also very sensitive to electron correlation effects. The large changes in the relative stabilities of both neutral and protonated species when including electron correlation contributions have dramatic effects on the calculated proton affinities. As shown in Table 2, the difference between MP2 and HF estimated values can be as large as 21.4 kcal/mol, while the difference between MP2 and G2(MP2) values is about 5 kcal/mol.

It is interesting to note that according to our theoretical estimations S_4 is slightly more basic than S_6 in the gas phase.

4. S_8 Protonated Species. One of the most conspicuous features of our experimental study is that S_8 was found to be a substantially stronger base than S_6. Unfortunately, a systematic survey of the S_8H^+ PES is completely beyond our computational capacity, mainly if one takes into account that, according to our previous discussion, a high level of theory is required if reliable description of the systems is sought for. Hence, we have limited our study to three different protonated species which differ in the size of the ring. The first one (**S8H**) corresponds to the structure which would be obtained by a protonation of the most stable S_8 crown structure of the neutral. The second one (**S7SH**) is a distorted seven-membered ring to which a SH^+ group is attached, and the third one (**S6S2H**) can be viewed as a distorted six-membered ring to which a S_2H^+ moiety is attached. The geometries of these three isomers, optimized at the HF/3-21G(d) level of theory, are given schematically in Figure 4. All of them were found to be local minima of the PES, at this level of theory, the **S8H** structure being the most stable. However, as expected in the light of our previous discussion, their relative stabilities change when electron correlation are taken into account, and at the MP2/6-31G(d)//HF/6-31G(d) level, isomer **S7SH** is found to be 2.0 and 4.5 kcal/mol more stable than **S8H** and **S6S2H**, respectively.

These electron correlation effects are clearly reflected in the calculated proton affinities. As it is shown in Table 4, if one considers only the three protonated species indicated above, S_8 is predicted to be much less basic than S_6, at the HF/6−31G-(d)//HF/3-21G(d) level of theory. When electron correlation effects are included at the MP2/6-31G(d) level, this gap does not change appreciably. However, when the basis set is significantly enlarged and the calculations are carried out at the MP2/6−311+G(3df,2p) level, the gap between the proton affinities of S_6 and S_8 disappears. We must then conclude that at this level it is not possible to offer a rationale of the enhanced basicity of S_8 with respect to S_6. Three different factors may be involved: (a) that the most stable protonated species is not the **S7SH** isomer, (b) that the optimized geometry of this isomer changes significantly when electron correlation effects are included stabilizing significantly this protonated form, and (c) that, as has been found for the other sulfur cycles, besides good geometries, a high level of theory is required to get reliable energetics. It is interesting to note however that **S7SH**, which resembles closely the global minimum of the S_6H^+ PES, in the

sense that it corresponds to a SH^+ group attached to a cyclic moiety, is found to be more stable than **S8H** species.

Conclusions

The gas-phase basicity of S_6 as determined by means of FT-ICR techniques is 167.8 kcal/mol, while S_8 is found to be significantly more basic (GB = 187.1 kcal/mol). A detailed analysis of the S_6H^+ PES using high-level ab initio techniques shows that the global minimum corresponds to a distorted five-membered ring structure, **1Hb**, while the chair-shaped six-membered ring protonated species **1Ha** lies 1.8 kcal/mol higher in energy. The agreement between the calculated and the experimental proton affinity values is very good, when the former are obtained at a sufficiently high level of theory. This can be taken as an indirect evidence that indeed the protonated form of S_6 corresponds to species **1Hb**. The situation is not so simple, however, and opens some intriguing possibilities. First, the energetic difference (1.8 kcal/mol) is comparable to the combined uncertainties originating in the experimental data and in the usual quality of the comparisons between experimental PAs and ab initio values. Second, the interconversion between both protonated species involves an appreciable activation barrier (≈20 kcal/mol), which, in principle, could prevent such interconversion in the time scale of the experiments. On the other hand, the formation of the encounter complex in the initial step of the proton transfer is able to provide a comparable amount of energy and thus overcome the barrier.

The characteristics of the S_4H^+ PES are rather different. The global minimum arises from the protonation of the cis open-chain isomer, which is the global minimum of the S_4 PES. This protonation processes, due to the high strain of the system, is followed by a S−S bond fission which yields the **3Hb** species. The lack of strain in this protonated form results in an enhanced stability of the system. Consistently, our G2-(MP2) calculations predict S_4 to be slightly more basic than S_6 in the gas phase.

A preliminary survey of the S_8H^+ PES indicates that, likely, the global minimum has similar characteristics to those found for the global minimum of the S_6H^+ PES, in the sense that both structures can be viewed as a SH^+ group attached to a cyclic sulfur moiety.

References and Notes

(1) See for instance, Taft, R. W.; Topsom, R. D. *Prog. Phys. Org. Chem.* **1987**, *16*, 1.

(2) Gal, J.-F.; Taft, R. W.; McIver, R. T. *Spectrosc. Int. J.* **1984**, *3*, 96.

(3) Alcamí, M.; Mó, O.; Yáñez, M.; Anvia, F.; Taft, R. W. *J. Phys. Chem.* **1990**, *94*, 4796.

(4) Abboud, J.-L. M.; Herreros, M.; Notario, R.; Esseffar, M.; Mó, O.; Yáñez, M. *J. Am. Chem. Soc.* **1996**, *118*, 1126.

(5) (a) Abboud, J.-L. M.; Herreros, M.; Notario, R.; Mó, O.; Yáñez, M.; Elguero, J.; Boyer, G.; Claramunt, R. *J. Am. Chem. Soc.* **1994**, *116*, 12486. (b) Abboud, J.-L. M.; Castaño, O.; Elguero, J.; Herreros, M.; Jagerovic, N.; Notario, R.; Sak, K. *Int. J. Mass Spectrom. Ion Processes* **1998**, *175*, 35.

Protonation of S_4, S_6, and S_8 Sulfur Cycles

J. Phys. Chem. A, Vol. 102, No. 41, 1998 **8003**

(6) Abboud, J.-L. M.; Herreros, M.; Notario, R.; Mó, O.; Yáñez, M.; Regitz, M.; Elguero, J. *J. Org. Chem.* **1996**, *61*, 7813.

(7) Abboud, J.-L. M.; Cañada, T.; Homan, H.; Notario, R.; Cativiela, C.; Díaz de Villegas, M. D.; Bordejé, M. C.; Mó, O.; Yáñez, M. *J. Am. Chem. Soc.* **1992**, *114*, 4728.

(8) Bordejé, M. C.; Mó, O.; Yáñez, M.; Herreros, M.; Abboud, J.-L. M. *J. Am. Chem. Soc.* **1993**, *115*, 7389.

(9) Bordejé, M. C.; Mó, O.; Yáñez, M. *Struct. Chem.* **1996**, *7*, 305.

(10) Bouchoux, G.; Dancourt, D.; Leblanc, D.; Yáñez, M.; Mó, O. *New J. Chem.* **1996**, *19*, 1243.

(11) Dance, I. G.; Fisher, K. J.; Willett, G. D. *J. Chem. Soc., Chem. Commun.* **1995**, 975.

(12) Schmidt, M.; Block, B.; Block, H. D.; Kopf, H.; Wilheim, E. *Angew. Chem., Int. Ed. Engl.* **1968**, *7*, 632.

(13) Laukien, F. H.; Allemann, M.; Bischofberger, P.; Grossmann, P.; Kellerhals, H. P.; Kopfel, P. In *Fourier Transform Mass Spectrometry, Evolution, Innovation and Applications*; Buchanan, M. V., Ed.; ACS Symposium Series 359; American Chemical Society: Washington, DC, 1987; Chapter 5, p 81.

(14) (a) Hernández-Laguna, A.; Abboud, J.-L. M.; Homan, H.; López-Mardomingo, C.; Notario, R.; Cruz-Domínguez, Z.; Haro-Ruiz, M. D.; Botella, V. *J. Phys. Chem.* **1995**, *99*, 9087. (b) Abboud, J.-L. M.; Castaño, O.; Della, E. W.; Herreros, M.; Müller, P.; Notario, R.; Rossier, J.-C. *J. Am. Chem. Soc.* **1997**, *119*, 2262.

(15) Abboud, J.-L. M.; Mó. O., de Paz, J. L. G.; Yáñez, M.; Esseffar, M.; Bouab, W.; El-Mouhtadi, M.; Mokhlisse, R.; Ballesteros, E.; Herreros, M.; Homan, H.; López- Mardomingo, C.; Notario, R. *J. Am. Chem. Soc.* **1993**, *115*, 12468.

(16) Hundreds of K_p values determined by this method in Prof. Taft's laboratory have been used in the construction of the databases given in ref 17.

(17) (a) Lias, S. G.; Liebman, J. F.; Levin, R. D. *J. Phys. Chem. Ref. Data* **1984**, *13*, 69 (b) Lias, S. G.; Bartmess, J. E.; Liebman, J. L.; Holmes, J. L.; Levin, R. D.; Mallard, W. G. *J. Phys. Chem. Ref. Data* **1988**, (Suppl. 1), *17*. (c) Hunter, E. P.; Lias, S. G. *J. Phys. Chem. Ref. Data* **1998**, *27*, 413.

(18) Bartmess, J. E.; Georgiadis, R. M. *Vacuum* **1983**, *33*, 149.

(19) Miller, K. J. *J. Am. Chem. Soc.* **1990**, *112*, 8533.

(20) (a) Parisod, G.; Gaumann, T. *Chimia* **1980**, *34*, 271. (b) McIver, R. T.; Hunter, R. L.; Ledford, E. B.; Locke, M.; Francl, T. J. *Int. J. Mass Spectrom. Ion Phys.* **1981**, *39*, 65.

(21) Frisch, M. J.; Trucks, G. W.; Schlegel, H. B.; Gill, P. M. W.; Johnson, B. J.; Robb, M. A.; Cheeseman, J. R.; Keith, T. A.; Peterson, G. A.; Montgomery, J. A.; Raghavachari, K.; Al-Laham, M. A.; Zakrzewski, V. G.; Ortiz, J. V.; Foresman, J. B.; Cioslowski, J.; Stefanow, B. B.; Nanayaklara, A.; Challacombe, M.; Peng, C. Y.; Ayala, P. Y.; Chen, W.; Wong, M. W.; Andres, J. L.; Replogle, E. S.; Gomperts, R.; Martin, R. L.; Fox, D. J.; Binkley, J. S.; Defrees, D. J.; Baker, J.; Stewart, J. P.; Head-Gordon, M.; Gonzalez, C.; Pople, J. A. *Gaussian 94* Gaussian, lnc.: Pittsburgh, PA, 1995.

(22) Raghavachari, K.; Rohlfing, C. M.; Binkley, J. S. *J. Chem. Phys.* **1990**, *93*, 5862.

(23) Quelch, G. E.; Schaefer llI, H. F.; Marsden, C. J. *J. Am. Chem. Soc.* **1990**, *112*, 8719.

(24) Molina, M. T.; Yáñez, M.; Mó, O.; Notario, R.; Abboud, J.-L. M. In *The Chemistry of Functional Groups. Supplement A3: The Chemistry of Double-Bonded Functional Groups*; Patai, S., Ed.; John Wiley & Sons: New York, 1997; Vol. 2, Chapter 23.

(25) Curtiss, L. A.; Raghavachari, K.; Trucks, G. W.; Pople, J. A. *J. Chem. Phys.* **1991**, *94*, 7221.

(26) Curtiss, L. A.; Raghavachari, K.; Pople, J. A. *J. Chem. Phys.* **1993**, *98*, 1293.

(27) Smith, B. J.; Radom, L. *J. Phys. Chem.* **1995**, *99*, 6468.

(28) Weinhold, F.; Carpenter, J. E. *The Structure of Small Molecules and Ions*. Plenum: New York, 1988 and references therein.

(29) Bader, R. F. W.; Essén, H. *J. Chem. Phys.* **1984**, *80*, 1943.

(30) Bader, R. F. W.; MacDougall, P. J.; Lau, C. D. H. *J. Am. Chem. Soc.* **1984**, *106*, 1594.

(31) Bader, R. F. W. *Atoms in Molecules. A Quantum Theory*; Oxford University Press: New York, 1990.

(32) Koch, W.; Frenking, G.; Gauss, J.; Cremer, D.; Collins, J. R. *J. Am. Chem. Soc.* **1987**, *109*, 5917.

(33) (a) Massart, D. L.; Vandenginste, B. G. M.; Deming, S. N.; Michotte, Y.; Kaufman, L. *Chemometrics: A Textbook*; Elsevier: Amsterdam, 1990; Chapter 2. (b) Guide for the use of terms in reporting data: *Anal. Chem.* **1982**, *54*, 157. (c) Freiser, H.; Nancollas, G. H. *IUPAC Compendium of Analytícal Nomenciature, Definitive Rules*, 1987; Blackwell Scientific Publications: Oxford, 1989; Chapter 2.

(34) Steudel, R. *Top. Curr. Chem.* **1982**, *102*, 149.

(35) Alcamí, M.; Mó, O.; Yáñez, M.; Abboud, J.-L. M.; Elguero, J. *Chem. Phys. Lett.* **1990**, *172*, 471.